# Experimental investigation of functional performance of a Vacuum Vessel Pressure Suppression System of ITER

D. Mazed[a], R. Lo Frano[a], D. Del Serra[a], D. Aquaro[a] and F.Orlandi[b]

[a]*Department of Civil and Industrial Engineering (DICI) - University of Pisa, Italy.*
[b]*General Electric oil & Gas, Firenze, Italy*

Important challenges for fusion technology deal with the design of safety systems aimed to protect the Vacuum Vessel (VV) from pressurizing accidents like the Loss Of Coolant Accident (LOCA). To prevent or mitigate structural damages, the solution proposed is a safety system able to quickly condense released steam in cold water at sub-atmospheric conditions. This water suppression tank (VVPSS) is so aiming at limiting the maximum pressure in the VV to 0.2 MPa during in-vessel coolant leak events and at maintaining the VV long-term pressure below atmospheric pressure during air or incondensable gases ingress, through the Direct Contact Condensation (DCC).

The novelty of this study resides especially in the working condition of VVPSS, which operates precisely to sub-atmospheric pressure: up to date no explicit experimental data or investigation of DCC are in fact available in literature. To overcome this lack an extensive experimental work has been done at DICI - University of Pisa, where numerous condensation tests (more than 300) were performed. The operation condition investigated took into account downstream pressure between 30 and 117 kPa and water pool temperature from 30 up to 85°C.

The experimental measurements allow to study the influence of steam mass flux, water temperature and pool pressure on the steam condensation phenomenon (and in turn, based on the stable condensation regime, correctly analyze the design parameter of VVPSS). The results obtained are presented and discussed. Innovative condensation regime maps are in addition provided.

Keywords: ITER, VVPSS, ICE event, steam condensation experiments

## 1. Introduction

Important challenges for fusion technology deal with the design of safety systems [1][2] aimed to protect the Vacuum Vessel (VV) from incident/accident situation, such as LOVA (Loss of Vacuum Event), ICE (Ingress of Coolant Event) [3][4][5]. When a category IV (extremely unlikely loading conditions [6] [7] corresponding to a single or multiple pipes break up to 0.6 $m^2$ flow area) leak scenario occurs, the water, at elevated temperature and high pressure, coming out from broken tubes evaporates into the VV resulting in over-pressurization.

A proposed solution to prevent/mitigate structural damages and to protect internal VV components consists in condensing efficiently the hot steam in a dedicated water suppression tank at sub-atmospheric pressure condition. This is obtained by means of a Vacuum Vessel Pressure Suppression System (VVPSS) [8]. In this way, the high steam pressure is strongly reduced because of the direct contact condensation (DCC) phenomena of its suppression tanks (STs).

In this study, the performance of the ST is investigated experimentally through the DCC of steam in cold water at sub-atmospheric pressure: steam condensation regimes are determined along with the identification of main parameters influencing possibly the design of VVPSS.

To highlight is that neither experimental nor analytical investigations of steam DCC at sub-atmospheric conditions, like those foreseen in ITER, have been yet reported despite the steam condensation was studied for atmospheric condition in the framework of Boiling Water Nuclear Fission Reactors [9][10][11] [12][13].

In what follows a brief description of the VVPSS and the role played by the Direct Contact Condensation will be given. In section 2.1, the experimental work done at the DICI of the University of Pisa to provide experimental data, necessary to allow a better assessment of DCC of steam phenomena will be presented. In section 3, results obtained are discussed.

## 2. Description of VVPSS in ITER

The VVPSS operates limiting the maximum pressure in the VV to 0.2 MPa during in-vessel coolant leak events and by maintaining the VV long-term pressure below atmospheric pressure during air or incondensable gases ingress. In this way, breach in the primary radioactivity confinement barrier is prevented.

The VVPSS consists of partially evacuated STs: three Large Leak Tanks (LLT's) and one Small Leak Tank (SLT). A relief pipeline connects the VV to the VVPSS Suppression Tanks. Each ST is partially filled of water to condense steam resulting from the most adverse water leakage into the Vacuum Vessel chamber [8] and to limit over-pressurization to about 150 kPa absolute.

STs have identical volume, inner diameter of 6.2 m and an overall height of about 4.7 m each. The LLTs contain about 60 $m^3$ of water each, whereas the SLT contains 40 $m^3$. Design parameters are set according to some

*author's email: rosa.lofrano@ing.unipi.it*

engineering considerations related to a ICE IV study carried out with MELCOR [14].

To manage its function, the ST is maintained under vacuum condition slightly above the saturation water vapor pressure at the prevailing temperature. The ST is designed to limit the final water temperature, after a loss of in-vacuum coolant event, to 95°C. Further details on the VVPSS are given in [8].

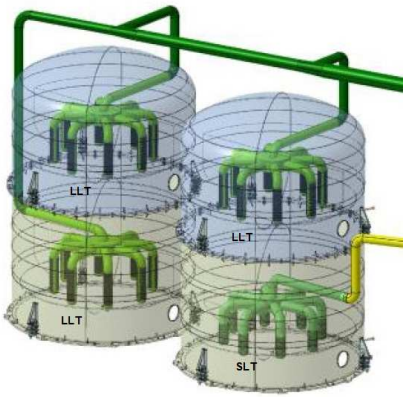


Fig. 1: View of ST with sparger [5][15].

### 2.1 Experimental test facility

*2.1.1 Scaling factor*

To evaluate the VVPSS performance and quantify the efficiency of steam condensation, an experimental facility was built at DICI of the University of Pisa of scaling factor 1/21 respect the ITER ST. The scaling factor was selected based on the need to functionally simulate the performance of the suppression tank without a modeling of the actual shape of the ITER system. The steam mass flux (calculated), the pressure and temperature are in a scaling factor of 1/1, respectively.

In the present experimental study, dimensions of the ST (called in the following Condensation Tank), such as the diameter and height, were determined as to the steam mass flux, the downstream pressure (in front of the hole), the water temperature and head level are equal to those in ITER.

*2.1.2 Structural components*

The test facility, schematized in the block diagram of Fig. 2, consists of:

- Superheated Steam Generator (SG);
- Flow Rate Control System (FRCS);
- Condensation Tank (CT);
- Auxiliary Tank System (AT);
- Vacuum System (VS);
- Heat Exchanger and Cooler System (HE plus Chiller);
- Degassed Water Supply System (DWT);
- Data Acquisition and Control System;
- Visualization and video recording system.

The main component of the facility is the CT, a 4.55 $m^3$ stainless steel cylindrical vacuum tight vessel of 1.4 m internal diameter, 8 mm thickness and 3.1 m overall height.

The SG consists of an electrical steam generator of 130 kW with a maximum steam mass flow rate of 45 g/s at a pressure of 1.49 bar and 130°C maximum superheating temperature. It produces water vapor from softened water fed at room temperature ($T_w$ ~ 20°C) and feeds the superheating module with water vapor at 110°C and 1.6 bar abs. The AT is designed to ensure steady state conditions prior to startup a test run [8].

Inside the CT the steam is injected through a removable sparger system (2" internal diameter) which is heated up by a resistance heater cable and thermally insulated so to reduce heat exchanges with the water of the tank. This will prevent steam flow losses through condensation on the sparger pipe internal wall.

The VS, made of a vacuum pump and the related loop, permit to create the vacuum pressure in CT and AT free space. The FRCS is made of two independent parallel feeding lines, each of which consists of one plug valve with pneumatic actuator-positioner and a steam mass flow rate transducer. This system allows to monitor and to control the steam mass flow rate during the test run.

Fig. 3 shows an overview of CT with indication of instrumentation, which is made of 28 thermocouples (TE) and 8 pressure transducers (PE). Four TE, mounted at 90°, and one PE are located at 8 different levels.

The physical parameters characterizing the DCC were recorded by means of a Data Acquisition System (DAS), equipped with LabVIEW©, and through a video recording system made of four high speed video cameras (GOPRO Hero4 model type) that were installed inside the CT.

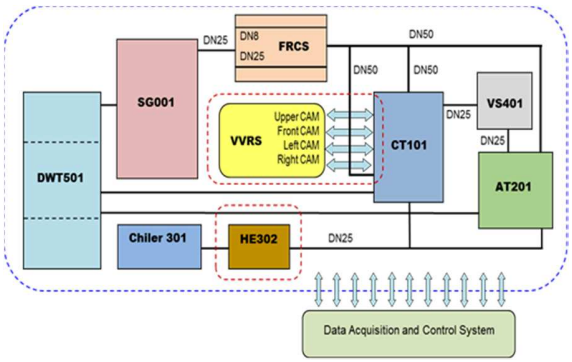


Fig. 2: Block diagram with experimental test facility subcomponents interconnected each other's.

The water is heated up directly by discharging superheated steam provided by the steam generator at full scale rate. Oppositely, the cooling down is obtained by

means of the Chiller or indirectly by means of the cold water flowing inside the internal AT coil piping.

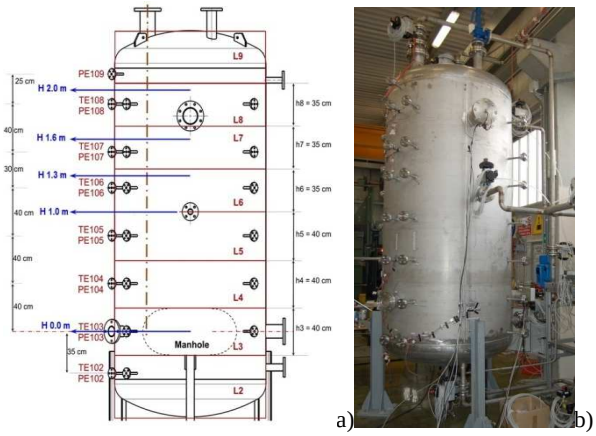


a) b)

Fig. 3 a, b: CT elevation scheme [8] (a) with indication of the levels and types of sensors (a) and view of the real experimental facility with cold and hot line, components and sensors (b).

## 3. Test matrix and results discussion

About 300 condensation tests were carried out in order to investigate the influence of steam mass flux, water temperature and pool pressure on the steam condensation regime (CR). Each test, for constant steam mass flow rate, lasts 900 s; for each sparger configuration.

In order to establish the steady state regime, required by the test conditions, the steam flow was firstly conditioned within the AT and then injected into the CT through a removable single or multiple-holed (with 1, 3 or 9 holes) sparger system [8].

The steam is fed through two lines (work ranges 0.30 - 7.5 g/s and 5 - 45 g/s, respectively) that are monitored with the FRCS through Coriolis and vortex mass flow meter and control valves.

The developed test matrix combines:

- Initial water or pool temperature ($T_W$): 30°C - 85°C;
- Downstream pressure ($P_W$): 30 kPa - 117 kPa;
- Steam mass flux ($G_S$): 30 - 160 kg/m$^2$s.

These parameters influence the behavior of the condensing steam jet, specifically: the vapor core or steam cavity, the mixing region, with vapor and water entrainment, and the turbulent jet region.

For any test, the increase of the water temperature (longitudinal and radial profiles) of the pressure in the vacuum space above the water head and the jet shape allow to characterise the condensation regimes and the heat transfer processes is taking place into the water mass.

In doing that, a significant role is given by the recorded video (Fig. 4) of the thermal mixing, induced by the steam discharge in the water tank, that permits to determine the stable or unstable steam condensation.

Fig. 4 shows the steam jet zone, whose maximum longitudinal extension is about 10 cm; the turbulent and mixing regions, where convective motion takes place, has a maximum horizontal extension of about 40 – 60 cm. Beyond this region, in horizontal and vertical directions, extend stagnant water regions, where the heat transfer phenomena occur mainly via diffusion.

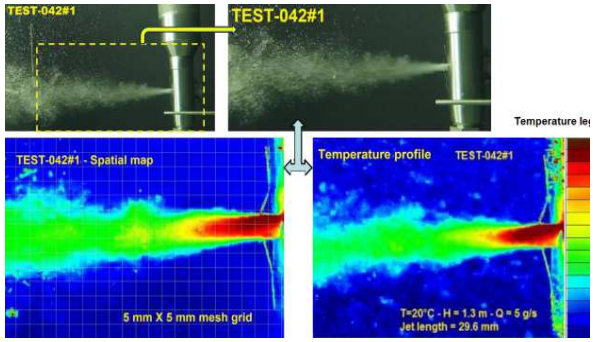


Fig. 4: Example of digital image processing for the determination of the condensing jet plume characteristics.

A reliable methodology to elaborate experimental data was developed by analogy to that of Song et al. [9]: to the aim, we performed experiments at atmospheric pressure (P = 106 kPa). The very good agreement between obtained data and those available in literature (Fig. 5) allowed identifying the shape of the steam jet plume for each condensation regime that are:

- Chugging (C);
- Transitional Chugging (TC);
- Condensation Oscillation (CO);
- Stable Condensation (SC);
- Bubbling Condensation Oscillation (BCO);
  Interfacial Oscillation Condensation (IOC).

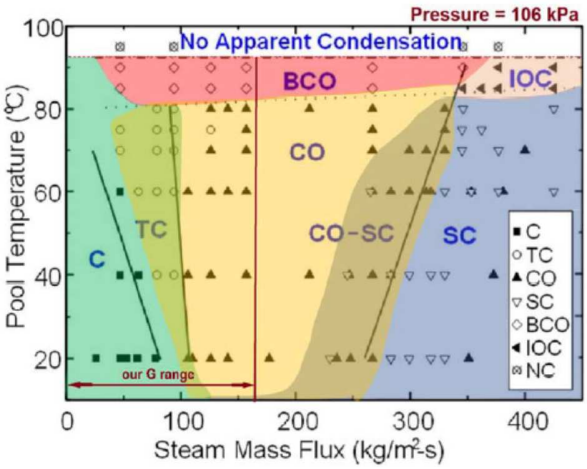


Fig. 5: Comparison between DICI data (condensation region are colored) and Song et al. (2012) (experimental data are given through geometrical symbols, whose legend is on the bottom right) data on a condensation regime map. The downstream pressure is also indicated for clarity.

Fig. 6 shows how the steam jet is influenced by the different sparger's configurations, temperature (widening of turbulent and mixing regions) and amount of vapor flowing into the suppression tank.

As the $P_W$ amplifies e.g. of a factor 2, at constant water temperature, the right CR boundary extends of almost the same proportion. At 50° C we shift from C to TC.

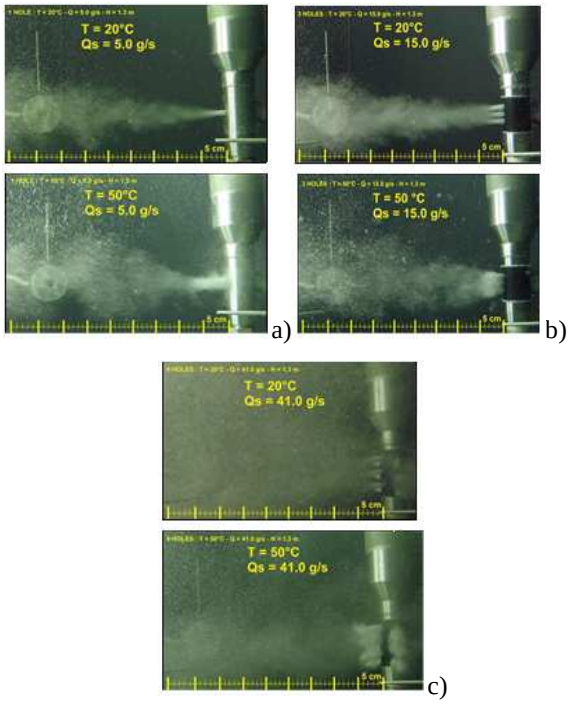


Fig. 6: Temperature effect on the condensation regime with injection of steam through a sparger with 1 hole (a), 3 holes (b) and 9 holes (c). The steam mass flux ($G_s$) per single hole is equal to the overall steam at sparger inlet subdivided the hole area ($G_s = Q_s / A_{hole}$)

Based on that, it is therefore possible to say that the steam condensation regime in water is mainly governed by the water temperature ($T_W$), the unit steam mass flow rate ($G_S$) and the downstream pressure in front of the sparger holes ($P_W$).

All the experimental data and, consequently, each correlated condensation regime can be represented in a ($G_S/P_W$, $T_W$) plane.

Condensation regions (and boundaries), in the 2D map provided in Fig. 7, can be analytically identified by means of a set of linear equations relating the water ($T_W$) to the downstream pressure ($P_W$) and to the steam mass flux ($G_S$), like:

$$T_W = a\frac{G_S}{P_W} + b \qquad (1)$$

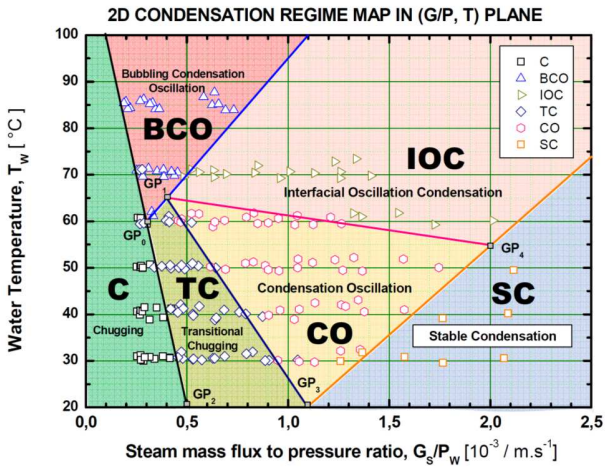


Fig. 7: Experimental CR map: each condensation region is identified with a different color a part form the proper nomenclature. $GP_i$ points identify the intersections of straights associated to each CR domain. Stable condensation appears at high $G_s/P_w$ ratio for $T_w$ from 30°C to 50°C.

Experimental results confirmed with high accuracy the capability of STs of the VVPSS to condense efficiently the injected steam (pressure increases gradually up to the saturation pressure determined by temperature).

## 4. Conclusion

From the experimental results on steam condensation at sub-atmospheric condition, we derive the following conclusions:

1) The ITER VVPSS is very effective in limiting the maximum pressure in the VV to 0.2 MPa during in-vessel coolant leak events and in maintaining the VV long-term pressure below atmospheric pressure during cat. IV event.

2) The condensation of steam through Direct Contact Condensation within the volume of cold water of the suppression tank is enhanced.

3) The steam mass flux to downstream pressure ratio is dimensionally homogeny to inverse velocity.

4) Six steam condensation regimes are identified. They are depending from the unit steam mass flux $G_S$, the downstream pressure $P_W$ and the water temperature $T_w$.

5) Downstream pressure has a determinant effect on the stability of steam condensation for fixed water temperature and steam mass flux.

6) Steam mass flux at stable condensation is lower of a factor 10 at sub-atmospheric pressure than that at atmospheric pressure.

It was concluded based on the experimental evidences of the present study that the ITER pressure suppression system is quantitatively very effective to reduce the pressurization due to in-vessel coolant leak events.

## Acknowledgments

We would also acknowledge DICI technicians for the valuable technical support provided in the experimental campaign.

## Reference

[1] R. Lo Frano et al., Thermo-mechanical test rig for experimental evaluation of thermal conductivity of ceramic pebble beds,

[2] D. Aquaro, Thermal mechanical analysis of a solid breeding blanket, Fusion Engineering and Design 9 (2003) (1-4 SPEC), pp. 511-518

[3] J. Carbajo et al., Modeling and analysis of alternative concept of ITER vacuum vessel primary heat transfer system, Fusion Engineering and Design, 85 (2010), pp. 1852–1858.

[4] M. Shibata et al., Experimental results of functional performance of a vacuum vessel pressure suppression system in ITER, Fusion Engineering and Design, 63-64 (2002), pp. 217-222

[5] R. Lo Frano et al., Fluid dynamics analysis of loss of vacuum accident of ITER cryostat, Fusion Engineering and Design, 109–111 (2016), pp. 1302–1307.

[6] IAEA, ITER Technical Basis, ITER EDA documentation Series No. 24, 2002.

[7] Guideline for ITER System Load Specifications, ITER_D_33TTPJ (private communication).

[8] D. Mazed et al., Experimental study of steam pressure suppression by condensation in a water tank at sub-atmospheric pressure, Proceedings ICONE24, June 26-30, 2016, Charlotte, North Carolina.

[9] C-H. Song et al., Steam Jet Condensation in a Pool from Fundamental Understanding to Engineering Scale Analysis, J. Heat Transfer, Transactions of the ASME-031004-2, 134, march 2012.

[10] J.C. Weimer et al., Penetration of vapour jets submerged in subcooled liquids, AIChE J., 19 (1973), pp. 552-58

[11] Seok Cho et al., Effect of multiple holes on the performance of sparger during direct contact condensation of steam, Exper. Therm. and Flui. Sci., 28 (2004), pp. 629-38.

[12] R. Redlinger et al., 3D-analysis of an ITER accident scenario, Fusion Eng. and Design, 75–79 (2005), pp. 1233-1236.

[13] K. Takase et al., Numerical study on direct-contact condensation of vapor in cold water, Fusion Engineering and Design 63-64 (2002), pp.421-428.

[14] Generic Site Safety Report, Volumes I–XI, ITER document Ref. G 84 RI, 2001

[15] ITER, VVPSS_Interim_Design_Report_SDJNS7_v2_2_29 January 2016 (private communication).